Advances in Science and Technology Research Journal

Advances in Science and Technology Research Journal, 2025, 19(1), 229–242
https://doi.org/10.12913/22998624/194887
ISSN 2299-8624, License CC-BY 4.0

Received: 2024.08.30
Accepted: 2024.11.15
Published: 2024.12.01

Simulation studies on the influence of clearances on the directional movement stability of articulated tracked unmanned ground vehicles

Mirosław Przybysz[1*], Tomasz Muszyński[1], Karol Cieślik[1], Karol Kończalski[1]

[1] Faculty of Mechanical Engineering, Military University of Technology, 00-908 Warsaw, Poland
* Corresponding author's e-mail: miroslaw.przybysz@wat.edu.pl

ABSTRACT

The article presents the results of simulation studies on the influence of clearances in the steering and track systems on the directional stability of articulated tracked UGVs (unmanned ground vehicles). The research was conducted using the MSC Adams multi-body system simulation environment. To this end, a model of an articulated UGV was developed, considering both the kinematics of the steering mechanism and the track system along with clearances and friction coefficients in the kinematic joints, as well as the track-ground interaction model. The study involved simulating maneuvers to avoid a selected set of obstacles. For this purpose, reference vehicle motion trajectories and corresponding steering control signals were developed. During the simulation studies, the clearance values of individual pairs of kinematic joints in the steering mechanism were varied, and parameters describing the motion of the UGV were recorded. The obtained results were compared with reference values. Simulation studies have shown that considering the backlash in the system results in significant deviations from the desired motion trajectory, reaching up to 80% of the measurement section for slalom between obstacles, and 18% in the case of an incidental avoidance of a single obstacle. The researched aspect is important, especially in terms of UGV control precision and motion stability. The results of the conducted research can provide guidance useful in the design of articulated tracked UGVs.

Keywords: UGV, articulated vehicle, directional movement stability.

INTRODUCTION

The minimization of threats to human health and life during the performance of various hazardous tasks has led to an increasing search for technical means and devices that can assist or even replace humans in carrying out these tasks [1]. These tasks are often conducted in difficult terrain conditions where vehicles cannot be used, leading to the deployment of Unmanned Ground Vehicles [2, 3]. This applies to both civilian and military applications [4].

By design, UGVs are utilized in challenging terrains and hazardous conditions. They can be controlled remotely, in a teleoperation system, semi-autonomously, or in "follow me" mode [1, 3, 5, 6]. This means that, unlike automotive vehicles, humans do not control them directly from onboard, which further increases the requirements they must meet [3].

One of the key aspects that influence the effectiveness of UGVs is their ability to move through terrain, generally referred to as off-road mobility. Several factors affect off-road mobility, including the range of movement speeds, the ability of UGVs to overcome terrain obstacles, the tractive forces developed by the drive systems, rollover stability, and maneuverability [7–14]. This creates a spectrum of functions and potential capabilities that have recently been the subject of extensive research.

As it is increasingly anticipated that within the next decade, the control of UGVs will be significantly more autonomous, a critical research problem is their capability to navigate predetermined paths with minimal deviation from the designated trajectories. The mechanical structure of the platform, particularly the characteristics of its steering system, predominantly influences this capability. Unlike automotive vehicles, due to the specific applications and differing requirements, UGVs practically do not use Ackerman steering systems. Exceptions include robotic commercial chassis that appear as manned vehicles, such as ATVs (All-Terrain Vehicle) and UTVs (Utility Terrain Vehicle) [15]. Currently, skid-steer systems predominate in many UGV solutions [4, 16]. The influence of their properties and factors affecting the platform's ability to follow predetermined paths has been relatively well studied. Research [17] has shown that one of the factors affecting the replication of the desired path is kinematic discrepancy. This can occur in both wheeled [17, 18] and tracked platforms [19]. Different dynamic radii of the wheels, resulting from variations in tire pressure or uneven load distribution among the wheels, cause the resultant path to deviate from the intended one despite attempts to synchronize their rotational speeds [20–22]. In extreme cases, even with a desired straight-line motion, significant deviations occur after traveling 30–50 meters [11, 13, 23]. This effect is mitigated in non-pneumatic wheels [24], where tire pressure cannot vary. In tracked chassis platforms, this phenomenon also arises from different pre-tension levels in the right and left tracks. In platforms weighing 500 kg or more, where hydrostatic drive systems with hydraulic motors directly driving each wheel are used [11, 17], deviations from the intended path are also linked to internal leaks within the drive system [17, 20, 22]. The properties of the terrain, particularly soil, on which the platforms operate, also significantly affect their ability to follow the designated trajectory. This mainly concerns varying coefficients of adhesion and the resulting slips between the wheels and the ground [18–20]. Given that soil properties and the skid-steer turning process itself are highly energy-intensive, on less cohesive soils, platforms may bury themselves while turning in place, losing their ability to complete the task. This is unacceptable in hazardous and crisis conditions for humans.

These factors have led to the use of articulated steering systems in UGVs. In this case, the steering process is significantly less energy-intensive and does not degrade the terrain, thereby greatly reducing the likelihood of the platform becoming immobilized compared to skid-steering. Since various possible configurations [25–27] of the steering joint position and the implementation of the steering mechanism exist, this increases the potential factors that can influence the UGV's ability to maintain the intended trajectory with such a system. Due to the required force to overcome steering resistance and the steering speed, hydrostatic steering systems dominate, whose properties also cause difficulties in maintaining the intended path [28]. Studies [25–30] using developed models have examined the impact of equivalent stiffness and damping in the hydraulic actuators of the steering system on the snaking process. Key parameters identified include hydraulic oil aeration, the diameter and length of hydraulic hoses, and the pressure within the steering system at any given moment. In [31], the influence of the gain between the operator and the actuator system on the directional stability of the platform with an articulated steering system was also determined.

This study focuses on the issue of UGVs following a designated path. Given the previously mentioned factors, the focus is on articulated steering systems. The results of previously published studies mainly address phenomena occurring within the hydraulic system itself, treating the mechanical structure of the steering joint as ideal, which constitutes a significant simplification. Therefore, this study presents the results of research on the impact of mechanical clearances in the kinematic pairs of the articulated steering mechanism of an unmanned ground vehicle on the accuracy of the UGV in following the designated path.

METHODS AND MATERIALS

The investigation was carried out utilising a simulation approach. The first step involves creating test tracks with obstacles representing different environmental conditions in which unmanned ground vehicles (UGVs) are expected to function.

Following that, a UGV simulation model was created based on the physical object "Dromader" and taking into account the steering system clearances. The clearance value of 0.1 mm was determined based on the measurement of the physical object.

Following this, evaluation indicators were developed to analyse the results of the simulation studies. In the final step, simulation studies were carried out in accordance with the adopted methodology, and an assessment was performed based on the predetermined evaluation indicators. The developed methodology was presented using a flowchart (Fig. 1).

Description of test tracks

For the purposes of the conducted research on the influence of clearance in the steering system of an articulated UGV on the resulting driving trajectory, a proprietary method was developed, taking into account various operational characteristics of the UGV:

Test I – Maneuvering between obstacles arranged along a line, requiring high-intensity operation of the steering system. The trajectory is described by a cosine function. The location of obstacles was determined based on an analysis of forested terrain. The distances between obstacles were set at $Dl_p = 2.6$ m, over a distance $l_p = 6 \cdot Dl_p$, The average diameter of the obstacles 350 mm and the amplitude $A = 2$ m (Fig. 2).

Test II – Avoiding a single obstacle lying in the path of the UGV and then returning to the original trajectory (Fig. 3). The trajectory is described by a function similar to tanh and consists of three segments: the first segment is the maneuver to avoid the obstacle $l_p' = 10$ m, the second segment is straight driving $l_p'' = 0.5$ m, and the third segment is the return to the original direction of travel $l_p''' = 12.5$ m. The entire maneuver is performed over a distance of $l_p = 23$ m, $A = 2.1$ mm The trajectory amplitude value was chosen to ensure a clearance of approximately 20% of the vehicle's width between the UGV and the obstacles being traversed. During the simulation studies, the displacement of the front (X_p, Y_p) and rear (X_t, Y_t) parts of the UGV was recorded at the intersection point of the longitudinal symmetry axis and the axis of the running gear, parallel to the ground plane XY (Fig. 4).

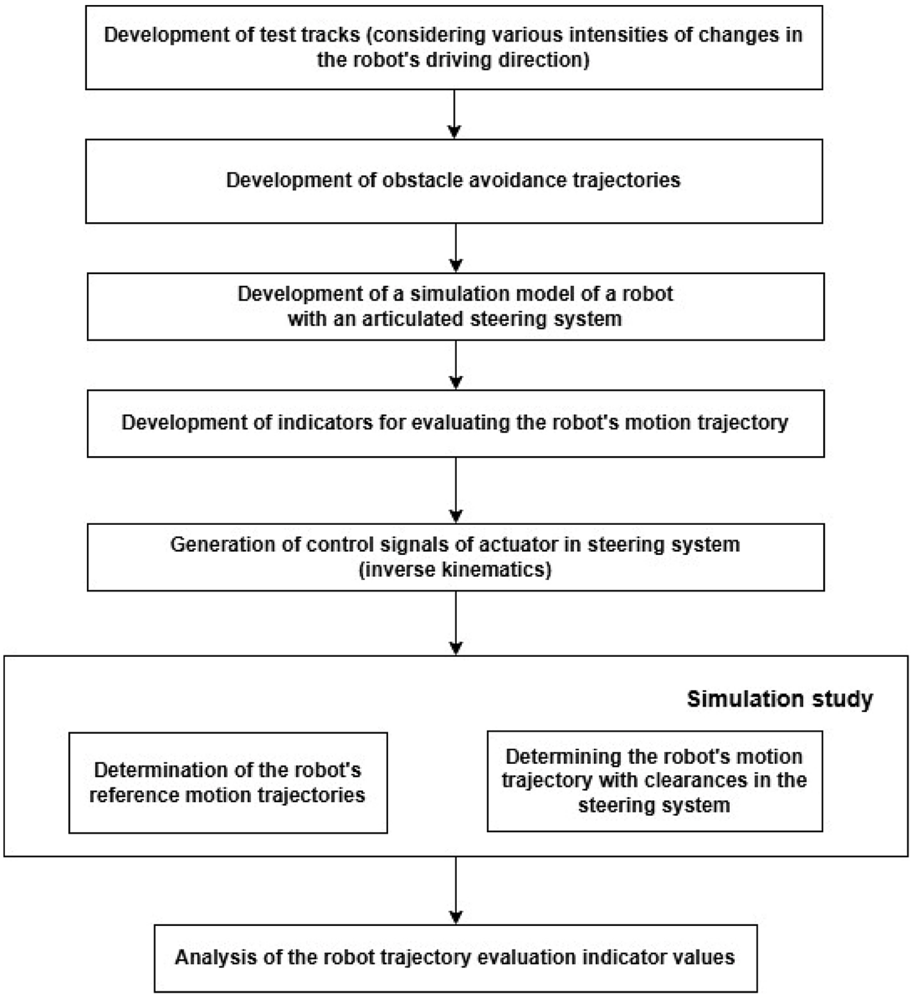

Figure 1. The flowchart of study methodology

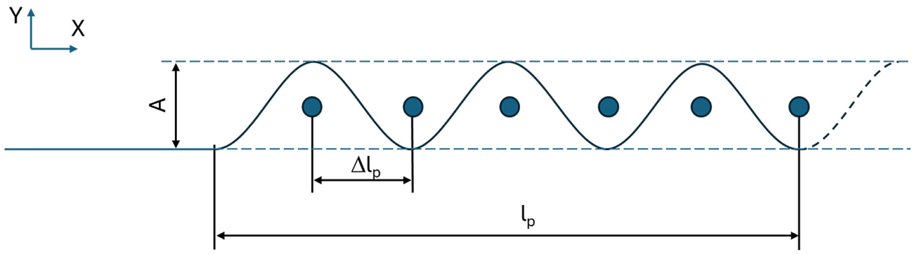

Figure 2. The trajectory of obstacle avoidance in Test I

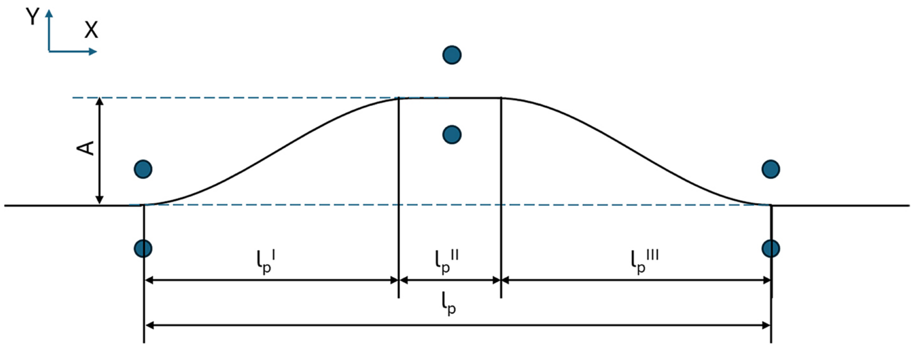

Figure 3. The trajectory of obstacle avoidance in test II

Model description

To conduct the simulation studies, a multibody model of a UGV with an articulated steering system was developed using the Adams View software. The model corresponded to the physical prototype of the articulated tracked vehicle "Dromader" (Fig. 5a). The geometric layer of the model was developed based on the CAD model of the UGV Dromader (Fig. 5b). The physical model consisted of simplified geometry that included the masses and mass moments of inertia of the individual elements, as well as their kinematic relationships. The basic parameters are presented in Table 1.

The following simplifying assumptions were used for building the model:

- The masses of elements significant for the resultant center of mass of the front and rear sections of the UGV were considered. The list of elements is presented in Table 2. The structural model is shown in Figure 7.
- The model was constructed from rigid bodies with constant density throughout their volume.
- The positions of the resultant centers of mass were determined based on the CAD model.
- A simplified contact model between the running gear and the ground was used, employing the impact force function (1).
- The influence of energy losses in kinematic joints and the drive system was neglected.
- The drive system used a differential mechanism, distributing power in parallel to four

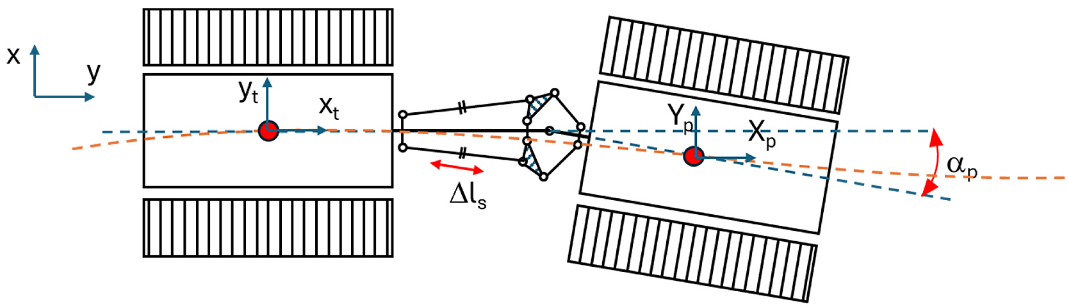

Figure 4. The position of trajectory recording for the front and rear parts of the UGV

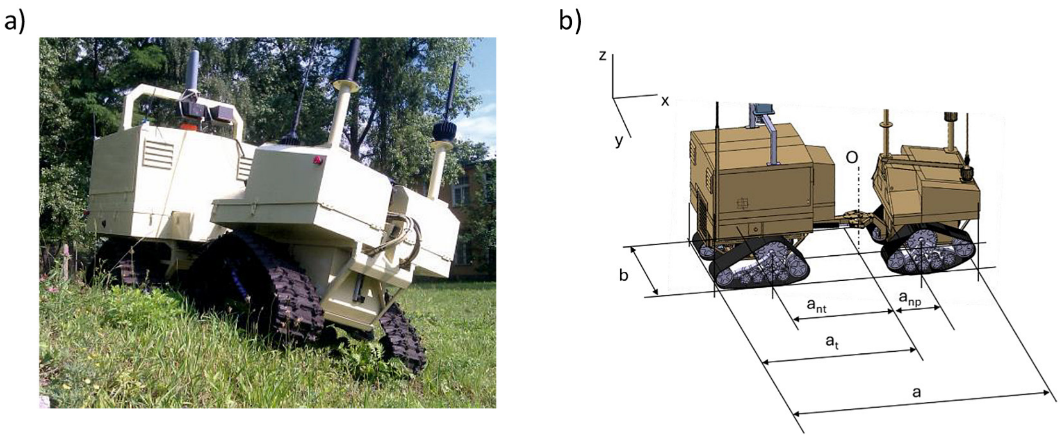

Figure 5. UGV "Dromader" with articulated steering: a) Physical object (own photo), b) CAD model

Table 1. Basic geometric parameters of the developed UGV Dromader model

Symbol	Name	Value, mm
a	Total length	2900
a_{nt}	Distance from the steering joint axis to the front track attachment axis	1040
a_{np}	Distance from the steering joint axis to the rear track attachment ax	580
a_t	Distance from the joint to the rear of the UGV	1700
b	Width	1124

track assemblies. A constant drive speed corresponding to 1 m/s was applied.

- In selected kinematic nodes, a clearance of 0.1 mm was applied, appropriate to the considered variant of the simulation model, by replacing the kinematic constraint with a force constraint representing contact between surfaces.

The developed model consists of two sections (1, 4), four track assemblies (2, 3, 5, 6), two levers (7, 8), two tie rods (9, 10), and two actuators composed of cylinders and pistons (11, 12, 13, 14) (Fig. 6).

The structure of mutual connections is shown in Figure 7, while the list of masses and mass moments of inertia is presented in Table 2

A simplified impact force contact model was used for the interaction between the running gear and the ground, accounting for static and dynamic friction coefficients with increasing slip velocity (Fig. 4).

$$F_{IMPACT}(x, \dot{x}, x_1, k, e, c_{max}, d) \tag{1}$$

where: x – the distance between model elements, $\dot{x}$ – the relative velocity between two elements, x_1 – the minimum distance between elements at which the normal contact force – F_{IMPACT} is not yet calculated, k – the stiffness of the interaction between the surfaces of the elements, e – the exponent of the normal contact force characteristic, c_{max} – the maximum damping value of the

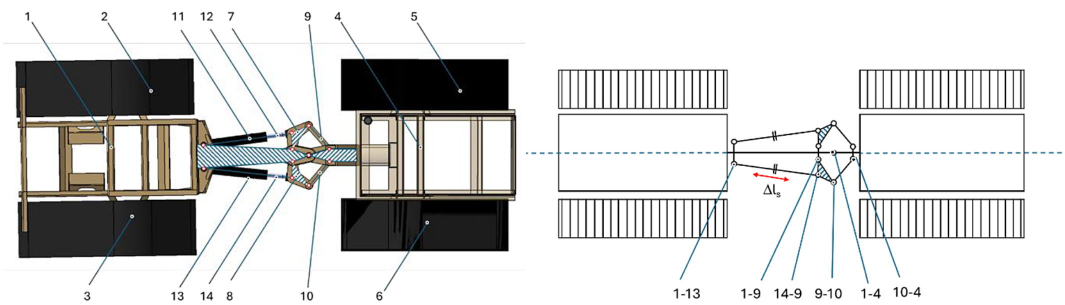

Figure 6. Components of the UGV Dromader model and kinematic connections

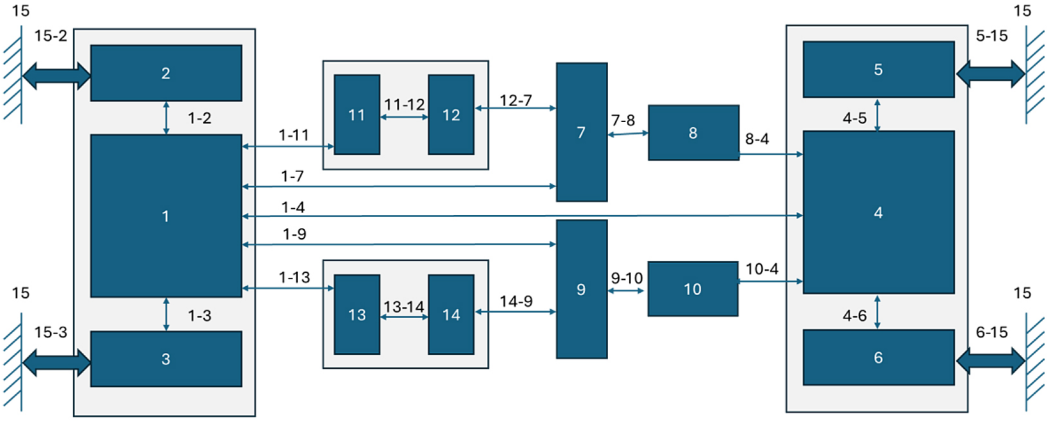

Figure 7. Diagram of the structure of kinematic and force connections

Table 2. Masses, mass moments of inertia of model elements and description of constraints

Masses and mass moments of inertia of model elements			
Symbol	Name	Mass, kg	Mass moment of Inertia: I_{xx}, kg·mm^2; I_{yy}, kg·mm^2; I_{zz}, kg·mm^2
1	Rear frame	250	6.05E+007; 4.88E+007; 2.51E+007
2, 3, 5, 6	Track assemblies	20	1.56E+006; 8.05E+005; 8.05E+005
4	Front frame	250	5.612E+007; 4.59E+007; 2.28E+007
7, 9	Lever	1.5	6567.03; 6102.93; 1602.78
8, 10	Tie rod	1	3734.63; 3383.49; 487.17
11, 13	Actuator cylinder	2.5	1.30E+004; 1.30E+004; 490.15
12, 14	Actuator piston	1	8777.79; 8777.79; 42.88
15	Ground	-	-
Description of constraints			
Symbol		Type of constraint	
1–2, 1–3, 4–5, 4–6, 1–7, 1–9, 1–11, 1–13, 12–7, 14–9, 7–8, 9–10, 8–4, 10–4		Rigid or clearance rotary kinematic constraints	
11–12, 13–14		Linear kinematic constraints	
15–2, 15–2, 15–5, 15–6		Driving system to ground contact	

normal contact force, d – the penetration value of the surfaces of the two elements at which the maximum damping value c_{max} is applied. The value of the traction force depends on the normal force (1) and the relative slip velocity (Fig. 8).

Evaluation indicatorsTo evaluate the test results, indicators characterizing the trajectory were developed. In the case of Test I, these were the coordinates of the extreme points A_i. In the further analysis, these coordinates were used to calculate characteristics describing the deviation of the main path of the UGV with clearances in the articulated steering system compared to the reference trajectory:

- The edges of the main path represented by the functions $y'_{135}(x)$, $y'_{246}(x)$, $y''_{135}(x)$, $y''_{246}(x)$, determined based on the maximum values A_1, A_3, A_5, and the minimum values A_2, A_4, A_6.

a) $y'_{135}(x) = a_1x^2 + b_1x + c_1$, determined based on the points A'_1, A'_3, A'_5 $\in y'_{135}$, determined based on the points A'_2, A'_4, $A'_5 \in y'_{246}$

b) $y'_{246}(x) = a_2x^2 + b_2x + a_2$, determined based on the points A''_1, A''_3, A''_5 $\in y''_{135}$

c) $y''_{135}(x) = a_3x^2 + b_3x + c_3$, determined based on the points A''_2, A''_4, A''_5 $\in y''_{246}$

The average value of the functions $y'(x)$, $y''(x)$, serving as an indicator of the main direction of driving of the

- front part of UGV:

$$y'(x) = \frac{y'_{135}(x) + y'_{246}(x)}{2} \tag{2}$$

- and rear part of UGV

$$y''(x) = \frac{y''_{135}(x) + y''_{246}(x)}{2} \tag{3}$$

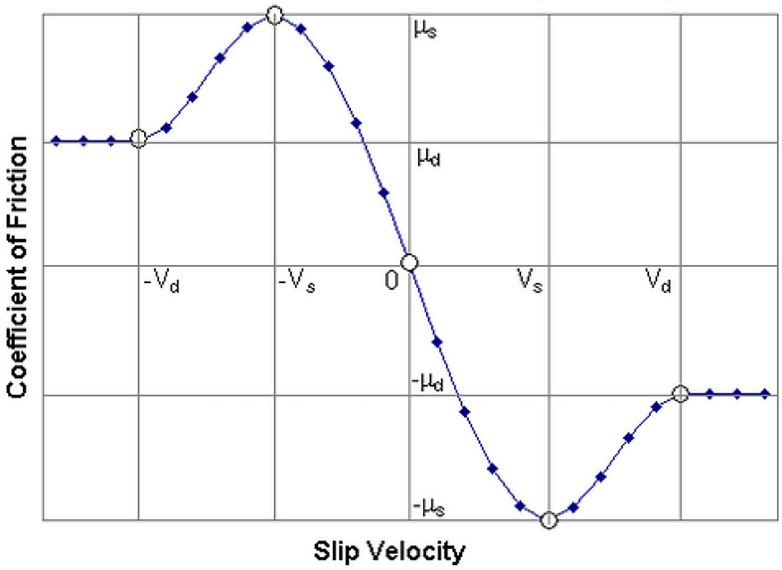

Figure 8. The friction coefficient as a function of slip velocity for the impact contact type [15]

The average value was used to determine the trajectory correction for comparing the amplitudes A'_{ik} and A''_{ik} (Fig. 9) of displacement relative to the main direction:

$$y'(x)_k = Y_t - y'(x) \tag{4}$$

$$y''(x)_k = Y_t - y''(x) \tag{5}$$

Additionally, the following parameters were adopted to evaluate the corrected characteristics $y'(x)_k$ and $y''(x)_k$:

- For Test I:
  - The relative error of the displacement amplitude values of the front part UGV A'ik relative to the reference amplitude:

$$\delta A' = 1 - \frac{A'_{ik}}{A'_a} \cdot 100\% \tag{6}$$

  - The relative error of the displacement amplitude values of the rear part of UGV A'ik relative to the reference amplitude:

$$\delta A'' = 1 - \frac{A''_{ik}}{A''_a} \cdot 100\% \tag{7}$$

  - The relative error of the maximum deviation value of the main path y'_{imax} from the straight-line path:

$$\delta y' = \frac{y'_{imax}}{y'_a} \cdot 100\% \tag{8}$$

The relative distance from the obstacle considered as the ratio of the distance from the obstacle to the width of the vehicle (the distance *r* determined on the simulation path)

$$\delta r'_i = \frac{r'_i}{B} \cdot 100\% \tag{9}$$

$$\delta r''_i = \frac{r''_i}{B} \cdot 100\% \tag{10}$$

- For Test II, the following was adopted to evaluate the results:
  - The difference between the maximum value of the trajectory deviation from the desired trajectory:

$$\Delta Y_{max} = Y_{iE} - Y_{aE} \tag{11}$$

The ratio of the maximum deviation value from the reference trajectory to the width of the UGV:

$$\delta Y_{max} = \frac{Y_{aE}}{B} \cdot 100\% \tag{12}$$

RESULTS AND DISCUSSION

The simulation study was conducted at a constant kinematic speed of the differential mechanism drive, from which the speed is further distributed in parallel according to the load to four running gear systems. This approach prevented the occurrence of circulating power within the system, which could lead to disturbances in the UGV's trajectory.

The study was divided into three stages. The first stage aimed to record the actuator movement in accordance with the planned trajectory. For this purpose, the front section of the UGV was kinematically linked to the reference trajectory, while the steering joint freely adjusted to the movement trajectory. At the same time, the actuator extension Δl_s was recorded during the drive.

In the second stage, the reference trajectory for the UGV was recorded without considering the clearances in the steering joint. For this purpose, the UGV chassis was kinematically released from the reference trajectory, and the steering was executed by implementing the recorded time course of the actuator extension Δl_s. In the third stage, the main study was conducted to assess the impact of clearances on trajectory deviations relative to the reference trajectory. The tests were performed similarly to the second stage, but with the addition of clearances in selected kinematic pairs of the steering joint. The study was conducted under the following variants (Fig. 9): a – without clearances (reference trajectory); b – clearances in all pins: (1–13, 1–9, 14–9, 1–4, 10–4) (Fig. 10); c – clearance in 1–4; d – clearance in 1–9; e - clearance in 14–9; f – clearance in 9–10; g – clearance in 10–4; h – clearance in 1–13. Example trajectories obtained from the simulation studies of the reference drive (variant a) and the variant with clearances (variant b) are presented in global XY coordinates (Figs. 9 and 10). The analysis of the results revealed a clear impact of the clearances in the steering joint system on the disturbances of the main path, described by the characteristics: y' and y''. Due to the significant similarity, where the trajectories of the front and rear part of the UGV overlap, the comparative analysis of the main path was limited to the trajectory of one part of the UGV (Fig. 10).

An example of the corrected trajectory adjusted for deviations from the main direction of drive is shown in Figure 11. It indicates that the sections of the UGV maintain a constant amplitude of movement, with the amplitude of the second section being 12% smaller than that of the front section in all cases: 100–104 mm.

The analysis of the corrected trajectory amplitude values A_{ik} indicates that the clearances in the steering system consistently caused a reduction in this value. Comparing the corrected amplitudes to the reference, the relative error had a constant value of approximately 4% for variant b, while in other cases, it did not exceed 1% (Fig. 12). The conducted analysis additionally allowed for determining the impact of clearances in the steering system on the distance from the obstacles for the front and rear sections of the UGV. Considering the dimensions of the obstacles (35 cm) between which the UGV performs the avoidance maneuver, and the vehicle width of 110 cm, it was found that the clearances did not have a significant impact on reducing the distance margin to the obstacles between the compared models. However, the effect is clearly visible when comparing the trajectory of the front and rear sections, resulting in a decrease in the distance from approximately 24% to 11–13% (Fig. 13).

The analysis of the relative errors of the corrected amplitude values Aik for the model considering all clearances (variant b) is significantly

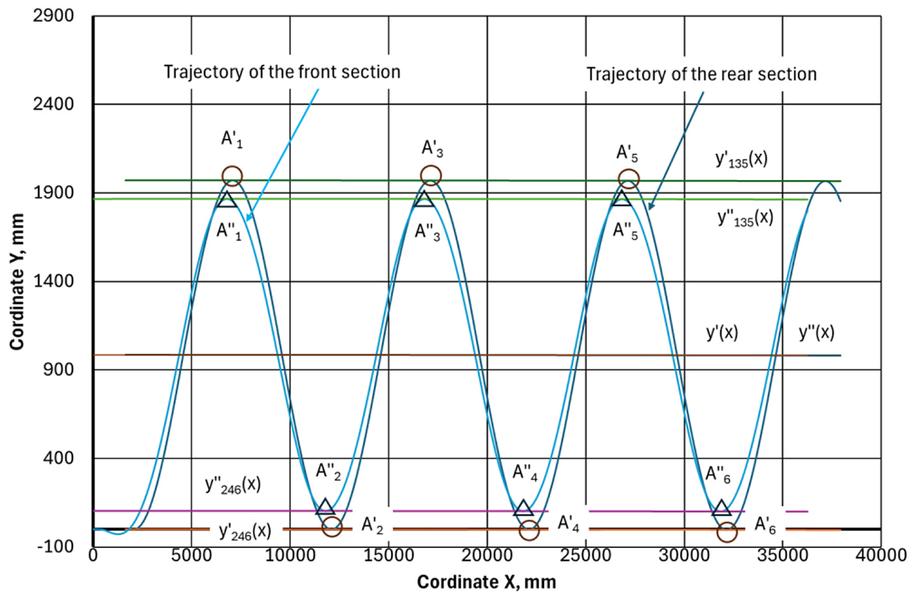

Figure 9. Reference trajectory for UGV with a steering system without clearances – variant a

greater (almost 9 times higher) than the relative errors of the other models with clearances (c-h) (Fig. 14). It should be noted that the relative error of the amplitude value A_{ik} for the model considering all clearances (variant b) does not equal the sum of the relative errors of the other models with clearances (c-h) and is twice as large as them, and it cannot be determined as the product of these errors. Based on this, it can be concluded that to evaluate the impact of clearances on trajectory accuracy, one should not use the individual errors directly but rather employ models that account for clearances in all joints. The studies indicate that accuracy is correlated with the distance of the connection relative to the steering axis in the joint – the larger this radius, the smaller the impact on trajectory error. The analysis of the main path deviation y' for variant b showed that the UGV collided with an obstacle (the fourth obstacle) after traveling approximately 22 meters (Fig. 14). In model d, the collision occurred after traveling twice the distance. In the other cases, no collision occurred over the considered section.

Table 3 presents the coefficients of the directional functions y', $y'=Ax^2+Bx$. The coefficient a in the function y′ indicates an increase in the angle of trajectory deviation – α from the

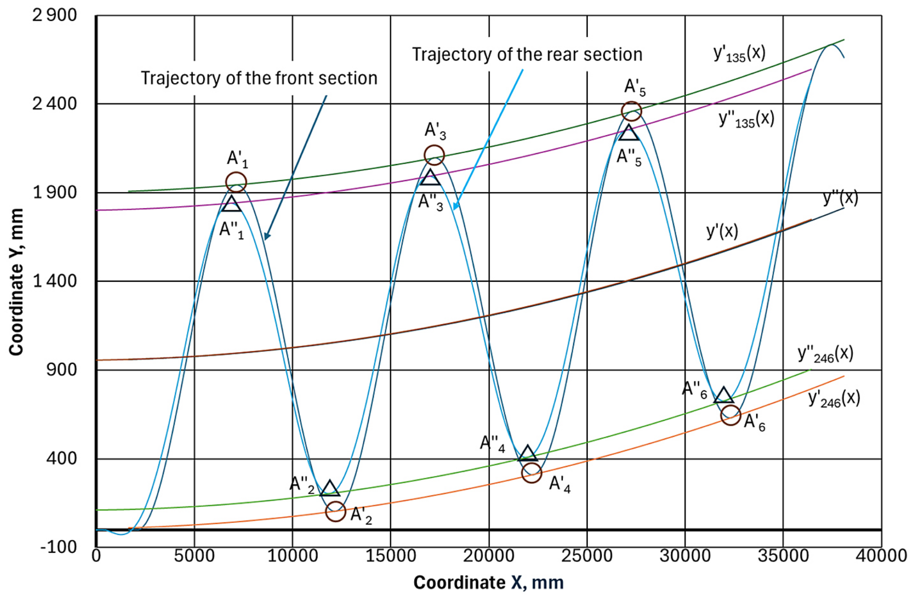

Figure 10. Reference trajectory for UGV with a steering system with clearances – variant b

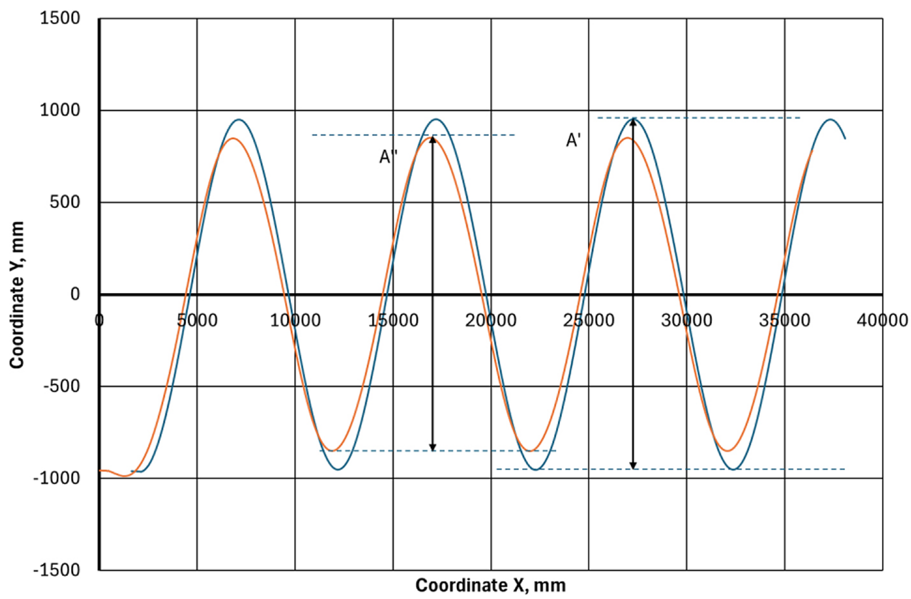

Figure 11. Corrected trajectory of movement for the UGV drive with clearances in the steering system

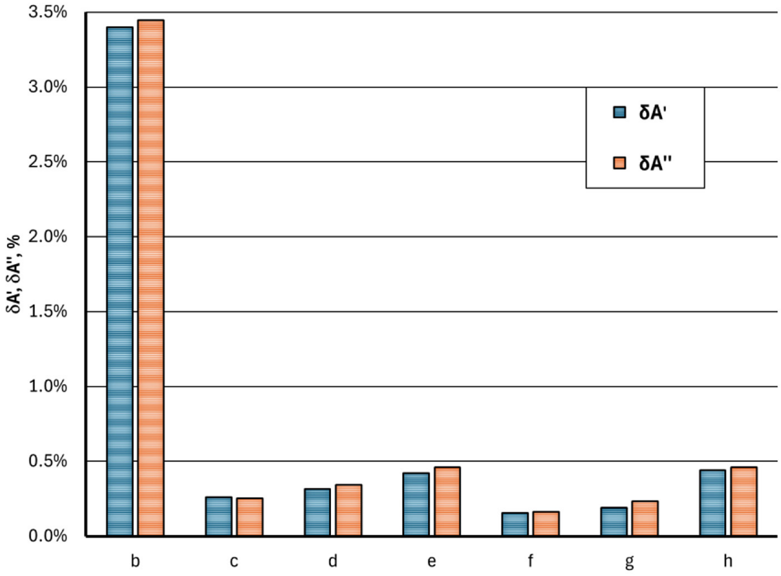

Figure 12. The relative value of the corrected amplitude error to the reference

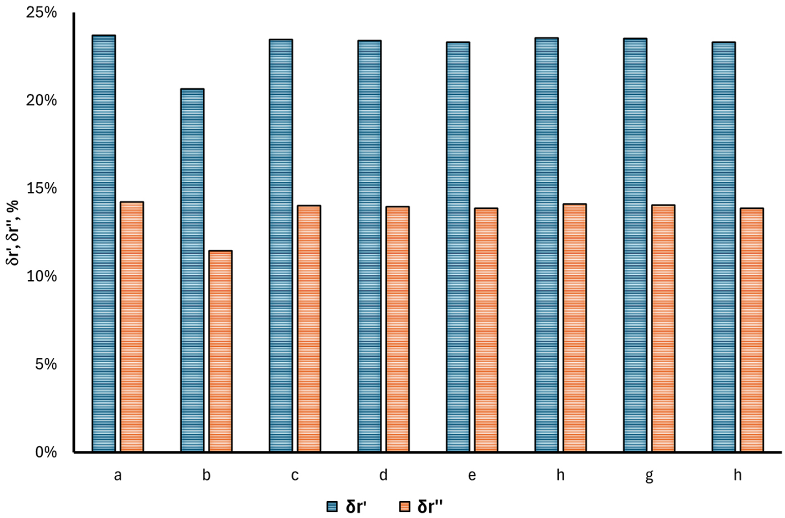

Figure 13. The relative distance value of the UGV structure to the passed obstacle

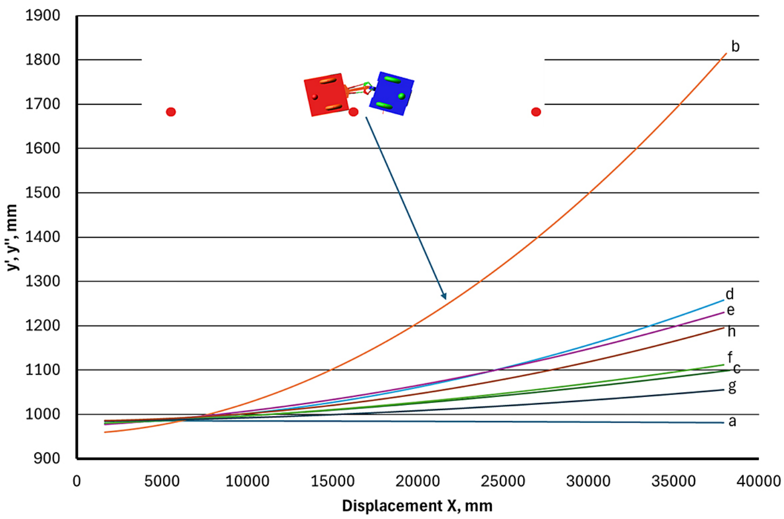

Figure 14. Characteristics y′ determining the main direction of travel for all considered model

Table 3. Coefficients A, B of the directional function y'

Parameter		Tested variants						
		b	*c*	*d*	*e*	*h*	*g*	*h*
Coefficients	*A*	5.541E-07	4.329E-08	1.802E-07	1.205E-07	5.877E-08	3.687E-08	1.385E-07
	B	0.0014476	0.0015496	0.0005263	0.0021982	0.0012992	0.0004954	0.0002900
The angle of trajectory deviation, °	*α*	0.0829450	0.0887866	0.0301597	0.1259493	0.0744389	0.0283859	0.0166188

reference with the driving distance of UGV. The coefficient b indicates a constant trajectory angle deviation resulting from dynamic interactions occurring only in the initial stage of the simulation. The comparison shows that dynamic interactions had a negligibly small impact on the angle of trajectory deviation - *α*, amounting to less than 0.12°. This translates to a trajectory error of 0.2% over the considered measurement section.

Comparison of the relative difference in the deviation of the directional function with respect to the desired trajectory at the end of the

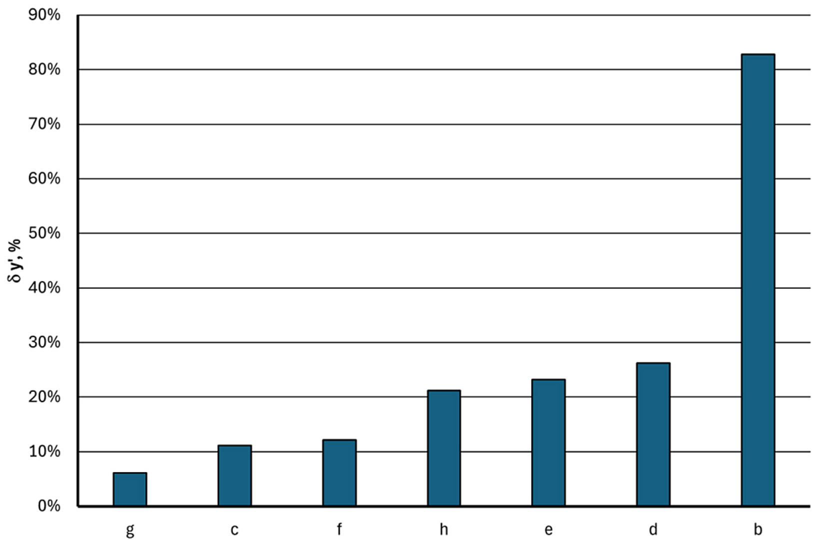

Figure 15. The relative error of the main movement trajectory for all models with respect to the reference trajectory measured at the end of the measurement section

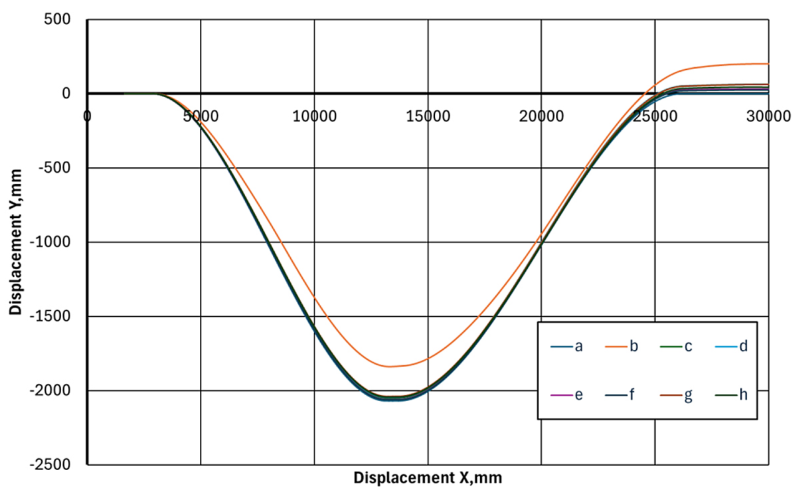

Figure 16. Trajectory of the UGV model while overcoming a single obstacle

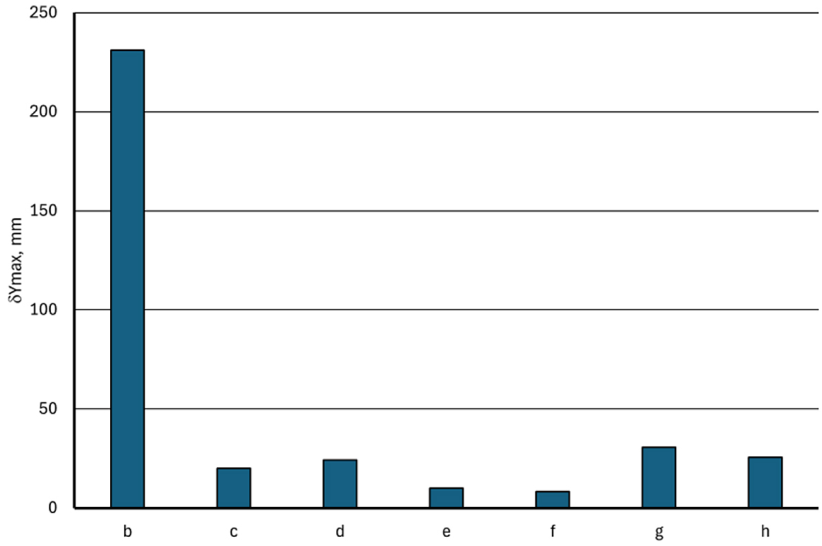

Figure 17. The deviation value of the trajectories of models b–h from the desired trajectory

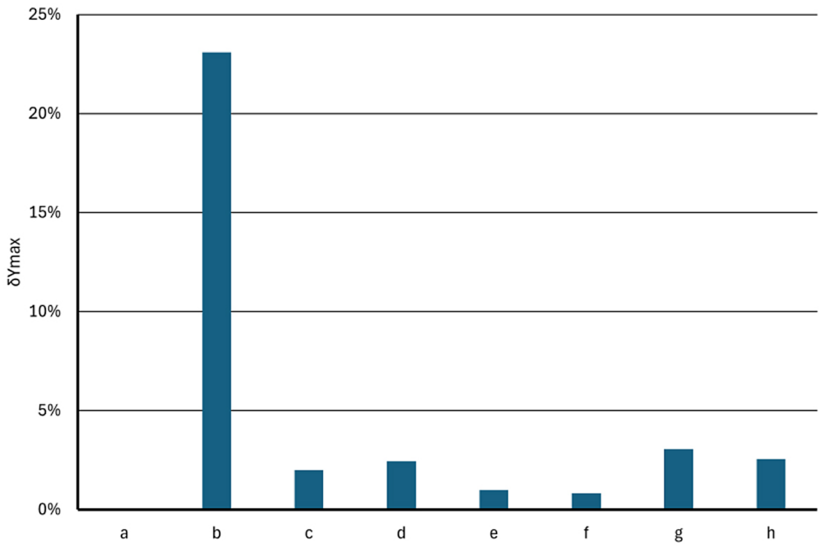

Figure 18. The impact of clearance in the steering system on the relative error value relative to the width of the UGV

measurement section indicates that, in the case of the steering joint with clearances in all pins, it is above 80%, whereas, in the case of clearances in individual pins, it does not exceed 25% (Fig. 15).

The trajectory study during the avoidance of a single obstacle was conducted according to the test II described in the methodology. Example results are presented in Figure 16. The analysis of the results used both the absolute and relative deviation values relative to the width of the UGV. The study indicates that the greatest deviation from the reference trajectory occurred in the variant b.

Comparing the obtained results, it was found that the maximum deviation from the desired direction after performing the obstacle avoidance maneuver for variant b was approximately eight times greater compared to the other models (Fig. 17). In the first case, it exceeded 200 mm, while for variants c-h, it averaged 25 mm. Comparing the deviation values of the trajectory relative to the width of the UGV, it was found that a single obstacle avoidance maneuver results in an error close to the assumed width margin of the corridor, amounting to approximately 18% (Fig. 18). In the other variants, the error did not exceed 6%. This indicates that after a single obstacle avoidance maneuver in the case of variant b, the error is close to the assumed width margin of the path.

CONCLUSIONS

The article presents the results of simulation studies on the influence of clearances in the steering system of an articulated UGV on deviations from the designated driving trajectory. For this purpose, a simulation model was developed in a Multibody environment, and a research methodology was created that takes into account movement in terrains requiring both high and low-intensity steering.

The studies indicate that these clearances in joins of the steering system have a particularly significant impact on the main movement direction. The deviation from the main movement trajectory that can be described as a quadratically function. In case of test I, the value of deviation from the desired direction at the end of the test track was about 80%. In the case of avoiding a single obstacle in the driving track (test II), the error of the movement trajectory was 18%.

Including clearances in all rotary joints resulted in more than three times the deviation from the designated trajectory compared to other variants, significantly accelerating the moment of UGV collision with an obstacle.

Clearances in the system did not have as significant an impact on changing the trajectory amplitude. The relative error for variant b was approximately 3.5%, while for the other models, it did not exceed 0.5%. The model took into account the play in the kinematic connections of the steering joint; therefore, the change in travel speed had no effect on the obtained errors of the motion trajectory. By additionally taking into account in the model the elastic-damping parameters of the flexible elements in the steering system and the running gear, the tests should be conducted taking into account different ranges of travel speeds.

Future research directions will include examining the impact of other factors on trajectory deviations from the designated path, such as the influence of the running gear, changes in the positions of the resultant centers of mass, and the characteristics of the steering system's actuators and control elements.

Acknowledgements

This work was financed/co-financed by the Military University of Technology under research project UGB 708/2024.

REFERENCES

1. Moorehead, S. Levels of autonomy control approach for mobile robots; proceedings of SPIE - The International Society for Optical Engineering, 2003.
2. Ni, J.; Hu, J.; Xiang, C. A review for design and dynamics control of unmanned ground vehicle. Proc. Inst. Mech. Eng., Part D: J. Automob. Eng. 2021, 235(4), 1084–1100.
3. Shimoda, S.; Kuroda, Y. Potential field navigation of high speed unmanned ground vehicles on Uneven Terrain. International Conference on Robotics and Automation, Barcelona, 2005.
4. Khan, R.; Malik, F. M.; Raza, A.; Mazhar, N. Comprehensive study of skid-steer wheeled mobile robots: development and challenges. Ind. Robot 2021, 48(1), 142–156.
5. Bloomfield, R. E. Autonomy, robotics, and dependability. IEEE Secur. Privacy Mag. 2015.
6. Mandow, J. L.; Martinez, J.; Morales, J. L.; Blanco, J. L.; Garcia-Cerezo, A.; Gonzalez, J. Experimental kinematics for wheeled skid-steer mobile robots. IEEE/RSJ International Conference on Intelligent Robots and Systems, San Diego, CA, USA, 2007, pp. 1222–1227.
7. Badar, T.; Backman, J.; Tariq, U.; Visala, A. Nonlinear 6-DOF dynamic simulations for center-articulated vehicles with combined CG. IFAC-PapersOnLine 2022, 55(14), 95–100.
8. Mokhiamar, O.; Amine, S. Lateral motion control of skid steering vehicles using full drive-by-wire system. Alexandria Eng. J. 2017, 56(4), 383–394.
9. Azad, N. L.; Khajepour, A.; McPhee, J. A survey of stability enhancement strategies for articulated steer vehicles. Int. J. Heavy Veh. Syst. 2009.
10. Lei, T.; Wang, J.; Yao, Z. Modelling and stability analysis of articulated vehicles. Appl. Sci. 2021, 8.
11. Łopatka, M.; Rubiec, A. Concept and preliminary simulations of a driver-aid system for transport tasks of articulated vehicles with a hydrostatic steering system. Appl. Sci. 2020, 17.
12. Daher, N.; Ivantysynova, M. Energy analysis of an original steering technology that saves fuel and boosts efficiency. Elsevier 2014.
13. Daher, N.; Ivantysynova, M. Yaw stability control of articulated frame off-highway vehicles via displacement controlled steer-by-wire. Elsevier 2014.
14. de Souza Mendes, A.; Ackermann, M.; Leonardi, F.; de Toledo Fleury, A. Yaw stability analysis of articulated vehicles using phase trajectory method. Int. Symp. Dyn. Probl. Mech. 2017.
15. Kończalski, K. Badania właściwości hydrostatycznego układu skrętu przegubowych bezzałogowych platform lądowych w systemie podążania za przewodnikiem. Doctoral Dissertation, Military University of Technology, Warsaw 2022.

16. Bartnicki, A.; Łopatka, M. J.; Muszyński, T. Szacowanie oporów skrętu burtowego wieloosiowych platform kołowych. Logistyka 2010.
17. Przybysz, M.; Łopatka, M. J.; Rubiec, A.; Krogul, P.; Cieślik, K.; Małek, M. Influence of hydraulic drivetrain configuration on kinematic discrepancy and energy consumption during obstacle overcoming in a 6 × 6 all-wheel hydraulic drive vehicle. Energies 2022, 15, 6397.
18. Beloousov, B.; Ksenevich, T.; Vantsevich, V.; Komissarov, D. 8×8 Platform for studying terrain mobility and traction performance of unmanned articulated ground vehicles with steered wheels. SAE Tech. Pap. 2013, 2013-01-2356
19. Cook, J. T.; Ray, L. E.; Lever, J. H. Mobility enhancement of heavy-duty tracked vehicles under load using real-time terrain characterization, traction control, and a towing winch. J. Dyn. Syst. Meas. Control 2019, 141(7), 071016.
20. Przybysz, M.; Rubiec, A. Identification Research of Wheels Angular Velocity Synchronization Accuracy for 6 × 6 Hydrostatically Driven Mobile Robot. Transp. Means Proc. 2017, 21st Int. Sci. Conf. Transport Means, Juodkrantė, Lithuania, 20–22 September 2017, 204–212.
21. Wang, Z.; Wang, P.; Liu, H.; Xu, D.; Guo, W.; Wei, W. Differential drive collaborative steering control of independent-wheel-drive articulated-steering electric vehicles for energy saving. IEEE Trans. Transp. Electrification 2024, 10(2), 4142–4158.
22. Gao, L.; Dong, Y.; Zhao, J. Dynamic modeling and characteristic analysis of articulated steering vehicles. Appl. Sci. 2023, 13(8), 5099.
23. Huang, B.; et al. Coordination Control of Active Steering and Direct Yaw Control for the Articulated Steering Vehicle. Shock Vibr. 2023, 2023(1), 5577119.
24. Jackowski, J.; Żmuda, M.; Wieczorek, M.; Zuska, A. Quasi-static research of ATV/UTV non-pneumatic tires. Energies 2021, 14, 6557.
25. Dudziński, P.; Skurjat, A. Impact of hydraulic system stiffness on its energy losses and its efficiency in positioning mechanical systems. Energies 2022, 15, 294.
26. Dudziński, P. Lenksysteme für Nutzfahrzeuge; Springer: Berlin/Heidelberg, Germany; New York, NY, USA, 2005.
27. Meng, Q.; Gao, L.; Xie, H.; Dou, F. Analysis of the dynamic modeling method of articulated vehicles. J. Eng. Sci. Technol. Rev. 2017, 10, 18–27.
28. Liem, D. T.; Huy, N. M.; Nam, L. V.; Nu, H. T. M. An adaptive predictor-based control approach for tracking control of a hydraulic actuator system. Adv. Sci. Technol. Res. J. 2024, 18(7), 419–436.
29. Jiang, W.; Luo, X.; Chen, X. Influence of structural flexibility on the nonlinear stiffness of hydraulic system. Adv. Mech. Eng. 2016, 8.
30. Gholizadeh, H.; Bitner, D.; Burton, R.; Schoenau, G. Modeling and experimental validation of the effective bulk modulus of a mixture of hydraulic oil and air. J. Dyn. Syst. Meas. Control 2014, 5.
31. Łopatka, M.; Muszyński, T. Research of the snaking phenomenon to improve directional stability of remote controlled articulated wheel tool-carrier. ISARC The Future Site 2003, 95.